

## Research on Complex Cepstrum Dereverberation of Partial Discharge Fault Direction Measurement in Transformer

Shijie Wang <sup>a</sup>, Wei Wang, Lizheng Wei, Jian Du, Lei Yu

North China Electric Power University, Beijing 102206, China;

<sup>a</sup>328799219@qq.com

### Abstract

Transformer insulation degradation is the main cause of partial discharge. Studying the accurate direction finding of partial discharge has important engineering significance for the safe operation of the entire power grid. The partial discharge signal is received by the fiber ultrasonic sensor array when partial discharge occurs. Due to the complicated structure of the transformer, the PD signal includes a PD signal that is reflected and scattered by a dielectric plane such as a tank wall, an iron core, or a winding. These reflected signals cause a large error in the direction of the local discharge point. The partial discharge direction finding experiment in oil was carried out based on the developed array, and the DOA of the discharge source was calculated by the MUSIC algorithm. The experimental results show that the minimum phase decomposition de-reverberation can effectively suppress the reverberation part of the PD signal. The accuracy of the direction finding after reverberation is significantly improved.

### Keywords

Partial discharge, dereverberation, fiber ultrasonic sensor, partial discharge direction-finding.

### 1. Introduction

The safe operation of power equipment is significant to ensure the safety of power grids. As the core of energy conversion in the process of power transmission and distribution, transformers are the most critical equipment in the safe operation of power grids. Its capacity and voltage level are also increasing with the construction of UHV power grids. Its operation is also related to the safety and economic operation of the power system. There are three types of faults in electrical equipment: mechanical faults, conductor faults, and insulation faults. From the statistical data, among the above three types of faults, the proportion of faults caused by insulation is the largest. Partial discharge is an important cause of insulation degradation of power transformers. Therefore, it is necessary to carry out on-line monitoring of the partial discharge of the power transformer to grasp the state of the insulation material in the real-time power transformer to avoid the occurrence of insulation failure [1-3].

When the partial discharge fault point direction in the transformer tank to be found, the ultrasonic signal, received by the fiber optic sensor includes, not only the direct part, but also many reverberant ultrasonic signals reflected by other paths., because of the reflection and scattering by the hard interface of the tank wall, the transformer winding and the iron core [4]. These reverberation signals can cause significant deviations in the direction of partial discharge faults inside the transformer tank. Therefore, it is necessary to carry out dereverberation studies on the local ultrasound signal.

Based on the partial discharge direction finding experiment in oil, the acoustical minimum phase decomposition method [5-11] is used to de-reverberate the partial discharge ultrasonic signal, which received by the EFPI sensor array. The processed partial discharge signal is direction-measured by using the MUSIC algorithm [12-18]. The experiment results show that the de-reverberation of the partial discharge signal by the minimum phase decomposition method can significantly improve the direction-finding accuracy. This provides a new method and idea for the accurate direction finding of partial discharge in high and low voltage windings of transformers.

## 2. Dereverberation principle

There are many methods for de-reverberation, such as classical and improved beamforming method, complex cepstrum filtering method, minimum phase decomposition method, Wiener filtering method [19] and so on. Among them, the minimum phase decomposition method is a popular de-reverberation method in recent years. Its de-reverberation effect is obvious. There is no limit to the number of sensors. Therefore, it is widely used in speech dereverberation. In this paper, the minimum phase decomposition method of each signal is used to reverberate, and then the MUSIC algorithm is used for the localization and direction finding.

### 2.1 Reverberation

The word "reverb" was first derived from acoustics. The sound wave propagates in a relatively closed space. The internal hard interface reflects the sound wave, and the absorption and attenuation of the audible sound wave by the hard interface are weak. Therefore, when the sound source continues to sound, the early sound waves are superimposed with the hard interfaces and the subsequent sound waves are superimposed. It causes "pollution" to subsequent acoustic signals. The "pollution" has a great influence on the degree of discrimination. This phenomenon is called reverberation. The sum of these non-direct signals is called a reverberation signal.

### 2.2 Reverberation model

The mathematical model of the reverb can be expressed by (1):

$$x[n] = u[n] + \sum_{k=0}^{\infty} \{ \rho_k s[n - kn_k] \} \quad (1)$$

Where  $s[n]$  is the pure ultrasonic signal emitted by the PD,  $n_k$  is the delay unit value of the ultrasonic signal after the  $k$  times reflection,  $s[n - kn_k]$  is the ultrasonic signal after the original ultrasonic signal has been reflected by  $k$  times,  $\rho_k$  is the reflection coefficient at the  $k$  time,  $u[n]$  is the noise signal in the current environment,  $x[n]$  is the sum of the ultrasonic signal that reaches the sensor directly and the ultrasonic signal that reaches the sensor through all other paths.

Ignoring the influence of the noise signal  $u[n]$ , according to the convolution property of the unit impulse function  $\delta(n)$ , the reverberation model represented by the equation (1) can be expressed into a convolutional form:

$$x[n] = s[n] * \sum_{k=0}^{\infty} \{ \rho_k \delta[n - kn_k] \} = s[n] * h[n] \quad (2)$$

Thus

$$h[n] = \sum_{k=0}^{\infty} \{ \rho_k \delta[n - kn_k] \} \quad (3)$$

Where "\*" donates convolution,  $h[n]$  donates impulse response in the fuel tank,  $h[n]$  is equal to the position  $kn_k$ , respectively, and each decay to the sum of a series of continuous impulse functions  $\delta(n)$  after  $\rho_k$  times the original amplitude. The reverberation signal  $x[n]$  is equal to the convolution of the tank impulse response  $h[n]$  with the pure generator point source signal  $s[n]$ . Therefore, the reverberation signal itself can be regarded as a kind of noise, which is not a common additive noise, but a convolution noise [11].

### 2.3 Minimum phase decomposition de-reverberation principle

According to the above analysis, the actual purpose of de-reverberation is to effectively separate the pure partial discharge ultrasonic signal  $s[n]$  from the transformer tank's impulse response  $h[n]$ . Finally, a pure partial discharge ultrasonic signal  $s[n]$  can be obtained. Thus, the problem of reverberation is transformed into the process of deconvolution of (2). The traditional complex cepstrum filtering de-reverberation method can convert the convolution relationship of  $s[n]$  and  $h[n]$

in the time domain into the additive relationship in the complex cepstrum domain.  $s[n]$  and  $h[n]$  are easier to separate on the complex cepstrum domain.

The calculation formula for  $x[n]$  complex cepstrum is as follows:

$$\hat{x}[n] = FFT^{-1}\{\log|FFT(x[n])|\} \tag{4}$$

Take the complex cepstrum transformation on both sides of (2)

$$\hat{x}(n) = F^{-1}[\ln X(\omega)] = F^{-1}[\ln H(\omega)] + F^{-1}[\ln S(\omega)] = \hat{h}(n) + \hat{s}(n) \tag{5}$$

In the cepstrum domain, the complex cepstrum of  $\hat{s}(n)$  is usually distributed near the origin, while  $\hat{h}(n)$  is distributed near the origin. Hence, a low pass filter can be utilized to filter out the effect of reverberation on  $\hat{h}(n)$ . After filtering the reverberated signal and then converting it into the time domain, the de-reverberation partial discharge ultrasonic signal can be obtained.

This method is relatively simple to implement. However, the relevant parameters of the low-pass filter window function are difficult to determine, and the calculation of complex cepstrum exists a phase ambiguity problem. The logarithmic phase of the product of two complex numbers does not satisfy the additive. So it is difficult to reconstruct the original signal.

The principle of minimum phase can be used to avoid the above problems. The detection signal received by the sensor can be decomposed into a minimum phase component and an all-pass phase component. The minimum phase signal is the signal that all pole zeros are within the unit circle, and it is also a causal signal. Since the pole zero of the minimum phase signal is near the time origin, the minimum phase signal in the complex cepstrum domain exhibits a prominent positive peak near the origin, followed by several exponentially decaying small amplitude peaks.

According to the Hilbert transform method, the complex cepstrum of the minimum phase signal is calculated as follows:

$$\hat{x}_{\min}(n) = \begin{cases} 2\hat{x}(n), & n > 0, \\ \hat{x}(n), & n = 0, \\ 0, & n < 0. \end{cases} \tag{6}$$

Where  $\hat{x}_{\min}(n)$  is the minimum phase component of the signal and  $\hat{x}(n)$  is the real cepstrum of the signal  $x(n)$ .

Reverb has little effect on the all-pass component, and its effect on the minimum phase is much more significant than the effect of the all-pass component. The all-pass component also contains the delay position information of the direct wave relative to the fault, mainly represented by the first positive peak on the complex cepstrum domain. Therefore, after decomposing the signal into the minimum phase component and the all-pass component, the minimum phase component of each sensor is passed through a low-pass filter to reduce the interference of the reverberation.

The de-reverberation algorithm based on the minimum phase decomposition complex cepstrum is mainly divided into three steps (as shown in Figure 1). First, the signal received by the sensor is decomposed in the frequency domain to obtain a minimum phase component and an all-pass component. Then, the minimum phase component is filtered. Finally, the all-pass component and the filtered minimum phase component are combined to obtain a de-reverberated signal.

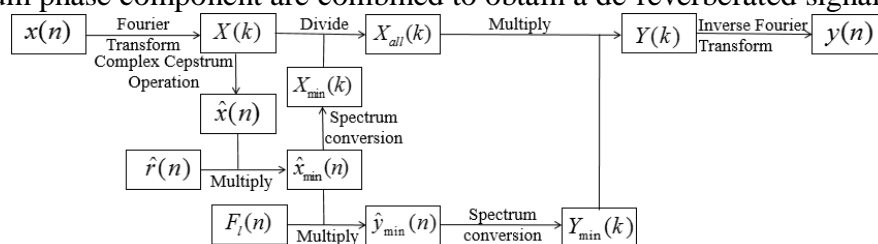


Figure 1 Minimum phase decomposition de-reverberation flow chart

In the figure,  $x(n)$  is the sensor receiving the PD signal. Windowing and framing preprocessing are performed on  $x(n)$ . Actually, the signal of one frame is processed.  $X(k)$  is a short-time spectrum of  $x(n)$ .  $X_{\min}(k)$  and  $X_{\text{all}}(k)$  are the minimum phase component of  $x(n)$  and the short-time spectrum of the all-pass component.  $\hat{y}_{\min}(n)$  and  $Y_{\min}(k)$  are the filtered minimum phase component in the complex cepstrum domain and in the frequency domain.  $F_l(n)$  is a low pass filter in the complex cepstrum domain.  $y(n)$  is the processed output signal.  $\hat{y}(n)$  is the real cepstrum of the signal  $y(n)$ .  $\hat{r}(n)$  is the complex cepstrum coefficient of the minimum phase signal. The values are as follows

$$\hat{r}(n) = \begin{cases} 2, & n > 0, \\ 1, & n = 0, \\ 0, & n < 0. \end{cases} \quad (7)$$

### 3. Spatial spectrum estimation

#### 3.1 3.1 Array signal model

Assuming that  $K$  far-field signals are incident on an array of  $M$  array elements, the signals received by the array can be expressed as:

$$X(t) = A(\theta, \varphi)S(t) + N(t) \quad (8)$$

Where  $X(t)$  is the sensor array receiving signal.,  $X(t) = [x_1(t), x_2(t), \dots, x_K(t)]^T$ ,  $S(t)$  is the signal vector,  $S(t) = [s_1(t), s_2(t), \dots, s_K(t)]^T$ ,  $N(t)$  is the noise vector,  $N(t) = [n_1(t), n_2(t), \dots, n_K(t)]^T$ ,  $A(\theta, \varphi)$  is the direction matrix of the signal. As shown in Figure 2,  $\theta$  represents the azimuth angle,  $\varphi$  represents the pitch angle, and  $(\theta, \varphi)$  represents the DOA of the signal.

$A(\theta) = [a(\theta_1, \varphi_1), a(\theta_2, \varphi_2), \dots, a(\theta_K, \varphi_K)]$ . Where  $a(\theta_i, \varphi_i)$  is the direction vector of the signal of  $(\theta_i, \varphi_i)$ :  $a(\theta_i, \varphi_i) = \exp(j2\pi f r k_i / v)$ ,  $i=1, 2, \dots, K$ .  $f$  is the signal frequency,  $r = [r_1, r_2, \dots, r_M]^T$ ,  $r_m$  is the coordinate of the  $m$  array element,  $k_i$  is the wave number vector of the signal of  $(\theta_i, \varphi_i)$ ,  $k_i = [\sin(\varphi_i)\cos(\theta_i), \sin(\varphi_i)\sin(\theta_i), \cos(\varphi_i)]^T$ .

#### 3.2 3.2 MUSIC algorithm

The MUSIC algorithm is called a multi-signal classification algorithm. It is a kind of spatial spectrum estimation algorithm. The basic idea is to feature decomposition of the covariance matrix of the array signal. Estimate DOA based on the orthogonality of the noise subspace and the signal direction vector.

The covariance matrix defining the array output signal  $X(t)$  is:

$$R = E\{X(t)X(t)^H\} = A(\theta)R_s A(\theta)^H + \sigma^2 I \quad (9)$$

Where  $R_s = E\{S(t)S(t)^H\}$ ,  $R$  is a positive definite Hermitain matrix. So

$$R = U_S \Sigma_S U_S^H + U_N \Sigma_N U_N^H \quad (10)$$

Where  $U_S$  is the signal subspace,  $U_N$  is the noise subspace,  $\Sigma_S$  and  $\Sigma_N$  is the corresponding diagonal matrix. Since the signal subspace and the noise subspace are orthogonal each other, then,

$$U_N^H a(\theta_k) = 0 \quad (11)$$

Where  $k=1, 2, \dots, K$

And the spatial spectrum function:

$$P_{music} = \frac{1}{a^H(\theta)U_N U_N^H a(\theta)} \tag{12}$$

From the above equation, find the peaks by  $\theta$  and  $\varphi$  changes to estimate DOA. The MUSIC algorithm direction finding spectrum and contour map are shown in Fig. 2.

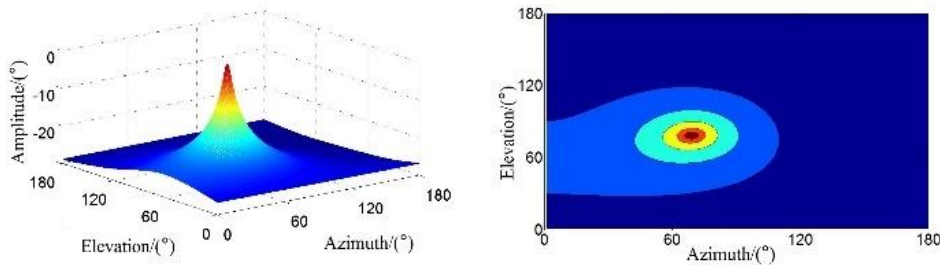


Fig. 2 MUSIC direction finding spectrum and contour map

The MUSIC algorithm is used to calculate the covariance matrix  $R$  of the array output signal  $X(t)$ . In fact,  $R$  is approximated by the first-order origin moment of a certain length of signal sequence

$$R = \frac{1}{L} \sum_{n=1}^L X(n) \tag{13}$$

## 4. Experiment research

### 4.1 Experiment platform

Establish a partial discharge direction experiment platform in oil, including simulated transformer tank, experimental transformer model and partial discharge model. The analog transformer tank is 200 cm × 100 cm × 150 cm and is filled with 25# transformer oil. The tank casing is grounded. The experimental transformer model is a 35KV transformer with a height of 0.6m, a high-voltage winding outer diameter of 0.24m, an inner diameter of 0.2m, a low-voltage winding outer diameter of 0.13m, an inner diameter of 0.1m, a transformer core height of 0.6m, and a radius of 0.1m, as shown in Fig. 3. The tip discharge model was selected in the experiment, and the needle plate electrode model was used, as shown in Fig. 4. Its high voltage electrode uses a brass tip. The distance between the high voltage electrode and the ground electrode can be adjusted according to the amount of discharge required. According to experience, when the distance between the high voltage electrode and the ground electrode is 1 mm, and the voltage is applied to about 10 kv, the signal of continuous partial discharge can be observed by the oscilloscope.



Fig. 3 Experimental transformer model

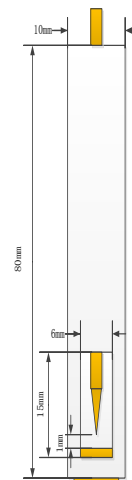


Fig. 4 Tip discharge model

### 4.2 Space three-dimensional coordinate system establishment

In this paper, four F-P fiber sensors are used to collect the PD signals. Four sensors are embedded in the mold and arranged in a counterclockwise arrangement, as shown in Fig. 5. Take the center point

of the mold as the origin  $o$  (0,0,0) of the three-dimensional coordinate system. The four sensor probes are in the  $xoz$  plane. Sensor probes No. 1 and No. 3 are located on the  $z$ -axis, and sensors No. 2 and No. 4 are located on the  $x$ -axis. The coordinates of the four sensor probes are (0,0,0.9), (0.9,0,0), (0,0,-0.9), (-0.9,0,0). The angle between the partial discharge source and the  $z$ -axis is defined as the elevation angle, which is denoted by the symbol  $\varphi$ . The angle between the projection of the partial discharge source on the  $xoy$  plane and the  $x$ -axis angle is defined as azimuth angles, which is denoted by the symbol  $\theta$ . Therefore, the direction of arrival DOA is expressed as  $(\varphi, \theta)$ , as shown in Fig. 6.

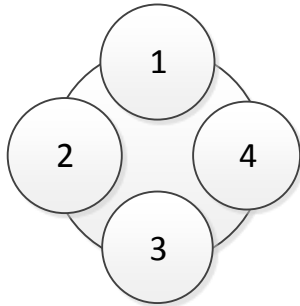


Fig. 5 F-P fiber sensor arrangement

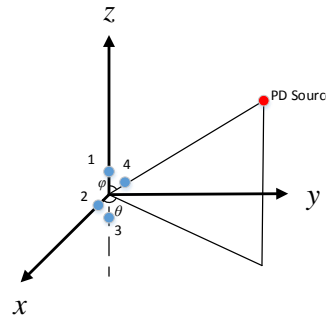


Fig. 6 Schematic diagram of spatial three-dimensional coordinate system

**4.3 PD source outside the high voltage winding of the transformer direction-finding**

Place the PD source between the high voltage winding turns, as shown in Fig. 7. The sensor array is placed in front of the transformer, 0.7m from the distance sensor. Since the sensor array needs to be mounted on the tank wall in the actual environment, the sensor array plane is designed to back to the tank wall and is 0.03 m away from the tank wall, as shown in Fig. 8. The PD source is set in different positions on the outside of the high voltage winding to collect the PD signal. The collected data is subjected to minimum phase method to reverberate and MUSIC direction finding. The results of the direction finding are directly compared with the results of the MUSIC direction finding without dereverberation.



Fig. 7 Placement of the PD source outside the high voltage winding

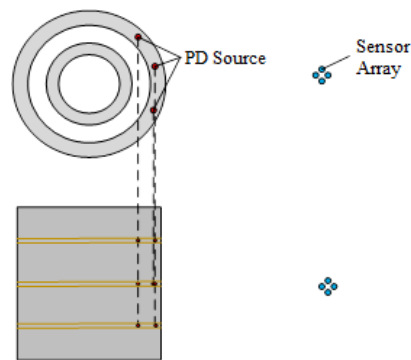


Fig. 8 Schematic diagram of partial discharge detection model for transformer high voltage outer winding

The actual coordinates, angles, and direction and error of the direction of the PD source in the three-dimensional coordinate system are shown in Table 1

The error is smallest when the source is facing the sensor array (the elevation and azimuth angles are  $90^\circ$ ). The farther the distance between PD source and the sensor array, the larger the direction-finding error. The main reason for the direct direction error is that there is a strong reverberation in the received partial discharge ultrasound signal. The main sources of reverberation are: 1) Since the sensor array is placed close to the tank wall, the sensor receives the partial discharge signal, reflected by the rear side wall. 2) When the PD source approach the tank wall, the path, PD signal goes directly



to the sensor array, is close to the refraction path through the tank wall, so that the reverberation contained in the signal received by the sensor. The reverberation affecting the first four sets of direct direction-finding errors is only due to the PD signal reflected by the tank wall on the rear side of the sensor array. The reverberation affecting the first four sets of direct direction-finding errors is only due to the PD signal reflected by the tank wall on the rear side of the sensor array. For the fifth set of experiments, the reverberation is from not only the PD signal reflected from the tank wall on the rear side of the sensor array, but also the PD signal reflected from the bottom tank wall. Therefore, the direct direction error of the fifth set of experiments is more than the direct positioning error of the first four sets of experiments.

Table 1 Discharge source coordinates and direction-finding results of outside the high voltage windings

Serial number	Coordinate	Actual angle / (°)	Direct direction finding / (°)	Direction finding error / (°)	Direction finding after reverberation / (°)	Direction finding error / (°)
1	[0,70,0]	(90.0,90.0)	(92.0,89.9)	2	(90.9,89.9)	0.91
2	[15 75 0]	(90.0,78.7)	(92.7,76.4)	3.5	(91.1,80.6)	2.1
3	[15 75 -12]	(98.9,78.7)	(94.5,82.4)	5.7	(95.8,80.5)	3.6
4	[15 75 12]	(81.1,78.7)	(85.6,82.1)	5.6	(84.3,80.6)	3.7
5	[15 75 -26]	(108.8,78.7)	(101.6,84.8)	10.1	(103.8,83.3)	7.5

**4.4 PD source inside the high voltage winding of the transformer direction-finding**

The PD source is placed inside the transformer high voltage winding, as shown in Fig. 9. The sensor array is placed above the transformer windings facing the oil passage. Sensor array plane is placed horizontally, as shown in Fig. 10.



Fig. 9 Placement of the PD source inside the high voltage winding

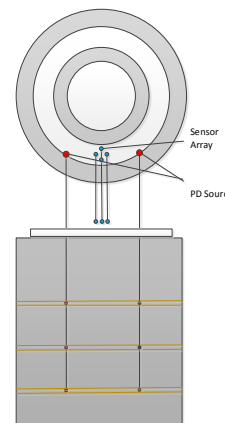


Fig. 10 Schematic diagram of partial discharge detection model for transformer high voltage inner winding

The actual coordinates, angles, and direction and error of the direction of the PD source in the three-dimensional coordinate system are shown in Table 2.

Because the inner structure of the transformer winding is dense and complex, the reverberation of the PD signal received by the sensor array is more than the outside of the transformer winding, resulting in positioning error. The farther distance between the source and the sensor array, the more reverberation of the PD signal is received by the sensor array through different reflection paths. Some signals even reflect the signal multiple times, resulting in a larger direction-finding error. After de-reverberation, the direction-finding accuracy is significantly improved. the more the reverberation, the more obvious the reverberation effect.

Table 2 Discharge source coordinates and direction-finding results of inside the high voltage windings

Serial number	Coordinate	Actual angle / (°)	Direct direction finding / (°)	Direction finding error / (°)	Direction finding after reverberation / (°)	Direction finding error / (°)
1	[2 8 -1]	(96.9,75.9)	(97.7,67.2)	8.7	(94.4,71.1)	5.4
2	[-1 8 -1.5]	(100.5,97.1)	(108.8,100.3)	8.9	(106.4,99.4)	6.3
3	[0 27 -1]	(92.1,90.0)	(95.2,99.5)	9.9	(96.5,96.5)	7.8
4	[14 27 4]	(82.5,62.6)	(94.0,61.8)	11.5	(91.7,61.8)	9.2
5	[4 35 -0.8]	(91.3,83.5)	(89.4,72.6)	11.1	(90.4,74.1)	9.4
6	[-8 35 -0.5]	(90.8,102.9)	(89.3,92.6)	10.4	(86.9,95.7)	8.2
7	[0 42 -1]	(91.4,90.0)	(79.2,95.7)	13.5	(81.6,95.0)	10.9

**4.5 PD source outside the low voltage winding of the transformer direction-finding**

The PD source is placed outside the transformer low voltage winding, as shown in Fig. 11. The sensor array is placed above the transformer windings facing the oil passage. Sensor array plane is placed horizontally, as shown in Fig. 12.

The actual coordinates, angles, and direction and error of the direction of the PD source in the three-dimensional coordinate system are shown in Table 3.

The partial discharge on the outside of the low-voltage winding of the transformer is similar to that on the inside of the high-voltage winding. Both of them are belong to the partial discharge of inner side of the transformer winding. The PD signal received by the sensor array has a large reverberation, and there is a large direction-finding error.



Fig. 11 Placement of the PD source outside the low voltage winding

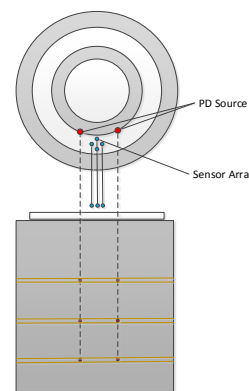


Fig. 12 Schematic diagram of partial discharge detection model of transformer low voltage outer winding

Table 3 Discharge source coordinates and direction-finding results of outside the low voltage winding

Serial number	Coordinate	Actual angle / (°)	Direct direction finding / (°)	Direction finding error / (°)	Direction finding after reverberation / (°)	Direction finding error / (°)
1	[1,13,1.5]	(83.4,85.6)	(78.5,90.7)	7	(78.7,88.5)	5.5
2	[11,13,3]	(80.0,49.8)	(86.0,45.8)	7.2	(85.0,46.7)	5.9
3	[1,22,1.5]	(86.1,87.4)	(81.6,80.8)	7.9	(82.5,82.4)	6.1
4	[1 35 1.5]	(87.5,88.4)	(91.6,96.4)	8.9	(84.2,94.2)	6.7
5	[13 35 6]	(80.9,69.6)	(74.1,77.5)	10.3	(77.4,76.3)	7.5
6	[3 50 1]	(88.3,86.6)	(76.5,84.9)	11.9	(79.4,86.6)	8.9
7	[9 50 2.5]	(87.1,79.8)	(81.0,68.7)	12.6	(80.3,73.5)	9.1



At the same distance, the direction-finding error of the partial discharge outside the high-voltage winding is larger than that inside the low-voltage winding. It is because that, the signal of partial discharge outside the high-voltage winding needs to pass through the cardboard. The PD signal will be distorted. It is influence on the accuracy of the direction-finding. After de-reverberation, the direction-finding accuracy is significantly improved. The more the reverberation, the more obvious de-reverberation effect. However, there are still some errors in the degree. The next step is to study the de-reverberation algorithm which improves the direction finding accuracy and the effect by appropriately increasing the number of array elements.

## 5. Conclusion

In this paper, the method of minimum phase decomposition de-reverberation of complex cepstrum is summarized. Based on fiber-optic ultrasonic sensor array and MUSIC algorithm, the partial discharge direction finding of transformer in oil is realized. To some extent, the problem of inaccurate direction-finding of partial discharge of the transformer is solved.

To improve direction-finding accuracy of the partial discharge of the transformer, the de-reverberation of the partial discharge ultrasonic signal is proposed. And the MUSIC algorithm is used for the direction-finding. Compared with the direct measurement using the MUSIC algorithm, the accuracy is significantly improved. The method is not only applicable to the partial discharge direction -finding outside the high voltage winding of the transformer, but also has good applicability to the partial discharge direction-finding inside the transformer (the inside of the high voltage winding and the outside of the low voltage winding).

## References

- [1] Al Saedi M A R, Yaacob M M. Partial discharge detection using acoustic and optical methods in high voltage power equipments: a review[J]. *Advanced Materials Research*, 2013, 845:283-286.
- [2] Si W R, Li J H, Li D J, et al. Investigation of a comprehensive identification method used in acoustic detection system for GIS[J]. *IEEE Transactions on Dielectrics & Electrical Insulation*, 2010, 17(3):721-732.
- [3] Sikorski W, Siodla K, Moranda H, et al. Location of partial discharge sources in power transformers based on advanced auscultatory technique[J]. *IEEE Transactions on Dielectrics & Electrical Insulation*, 2012, 19(6):1948-1956.
- [4] Masahiro Kozako, Hiroki Murayama, Masayuki Hikita, Kenji Kashine, Itaru Nakamura, Hidenobu Koide. On the Use of Acoustic Signals for Detection and Location of Partial Discharges in Power Transformers[J]. *IEEE International Conference on Condition Monitoring and Diagnosis*, 2012, 854 – 857.
- [5] Su Xianli. Research on speech dereverberation[D]. Sichuan I: Sichuan University, 2006.
- [6] A microphone array processing technique for speech enhancement in a reverberant space[J]. *Speech Communication* 18 (1996) 3 17-334.
- [7] Q.-G. Liu, B. Champagne, P. Kabal. Room Speech Dereverberation via Minimum-phase and All-pass Component Processing of Multi-microphone Signal[J]. *IEEE Pacific Rim Conference on Communications, Computers, and Signal Processing. Proceedings*, 1995, 571 – 574.
- [8] Ma Mingyu. Research on reverberation reduction of speech signal[D]. Xi'an Jiao Tong University, 2014.
- [9] Wu Jiadong, Chen Guangzhi. Principle and technologies of speech signal dereverbration [J]. *Audio Engineering*, 2006(05):63-67.
- [10] D. Cole, M. Moody, S. Sridharan. Intelligibility of reverberant speech enhanced by inversion of room response. *Proceedings of ICSIPNN '94. International Conference on Speech, Image Processing and Neural Networks*, 1994, 241 - 244 vol.1.
- [11] Lü Liang, Xin Xiaohu, Huang Guoqiang, *et al.* Design of re-locatable ultrasonic array and ultra high frequency combined sensor for partial discharge location in oil. *High Voltage Engineering*, 2014; 40(8): 2328—2334

- 
- [12] Luo Richeng, Li Werguo, Li Chengrong. A multi-target method to locate internal partial discharge sources within transformer based on array signal processing. *Power System Technology*, 2006; 30(1): 65—69
- [13] Xie Qing, Cheng Shuyi, Lü Fangcheng, *et al.* Location of partial discharge in transformer oil using circular array of ultrasonic sensors. *IEEE Transactions on Dielectrics & Electrical Insulation*, 2013; 20(20): 1683—1690
- [14] Xin Xiaohu, Luo Yongfen, Du Fei, *et al.* Comparisons of direction of arrival algorithms applied to ultrasonic arrays for partial discharge location in oil. *Proceedings of the CSEE*, 2015; 35(20): 5351—5359
- [15] Wang Yongliang, Chen Hui, Peng Yingning, *et al.* Theory and algorithm of spatial spectrum estimation. Beijing: Tsinghua Press, 2004: 253—273
- [16] He Zishu, Huang Zhenxing, Xiang Jingcheng. The performance of DOA estimation for correlated signals by modified MUSIC algorithm. *Journal on Communications*, 2000; (10): 14—17
- [17] Liu Yun, Li Zhishun. A new method for estimating DOA (direction of arrival) of wideband coherent sources. *Journal of Northwestern Polytechnical University*, 2003; 21(4): 457—460
- [18] Zhang Xiaofei, Chen Huawei, Qiu Xiaofeng. *Array signal processing and MATLAB implementation*[M]. Publishing House of Electronics Industry, 2015.
- [19] Zhang Dehui, Chen Guangzhi. A means based on wiener filtering for dereverberation in speech communication[J]. *Journal of Shanghai Jiaotong University*, 2009, 43(06):949—952